Bees, M.A., Hill, N. and Pedley, T.J. (1998) *Analytical approximations for the orientation distribution of small dipolar particles in steady shear flows.* Journal of Mathematical Biology, 36 (3). pp. 269-298. ISSN 0303-6812

http://eprints.gla.ac.uk/34648/

Deposited on: 24 August 2010

Enlighten – Research publications by members of the University of Glasgow
http://eprints.gla.ac.uk

J. Math. Biol. (1998) 36: 269–298

Analytical approximations for the orientation distribution of small dipolar particles in steady shear flows

M. A. Bees[1], **N. A. Hill**[1], **T. J. Pedley**[2]

[1]Department of Applied Mathematical Studies, University of Leeds, Leeds LS2 9JT, UK
e-mail: amt5mab@amsta.leeds.ac.uk
[2] Department of Applied Mathematics and Theoretical Physics, University of Cambridge, Cambridge CB3 9EW, UK

Received 10 February 1997; received in revised form 26 May 1997

Abstract. Analytic approximations are obtained to solutions of the steady Fokker-Planck equation describing the probability density functions for the orientation of dipolar particles in a steady, low-Reynolds-number shear flow and a uniform external field. Exact computer algebra is used to solve the equation in terms of a truncated spherical harmonic expansion. It is demonstrated that very low orders of approximation are required for spheres but that spheroids introduce resolution problems in certain flow regimes. Moments of the orientation probability density function are derived and applications to swimming cells in bioconvection are discussed. A separate asymptotic expansion is performed for the case in which spherical particles are in a flow with high vorticity, and the results are compared with the truncated spherical harmonic expansion. Agreement between the two methods is excellent.

Key words: Suspensions – Fokker-Planck Equation – Dipolar particles – Orientation distributions – Bioconvection

1 Introduction

In this paper, we consider the orientation probability density function (p.d.f.), $f(\boldsymbol{p})$, for a spheroidal particle with an asymmetric mass distribution, immersed in a general flow field. With a biological application to bioconvection patterns in mind, we assume that we can model all of the random fluctuations in orientation caused by external factors and by variations in particle geometry (i.e. variations in shape and variations due to the waving of cilia or flagella) as if they were generated by rotational Brownian motion and can be represented by one coefficient called the effective rotational diffusivity, D_r. Jones et al. (1994) investigate the explicit effects of bi-flagellated swimming and conclude that only small quantitative changes are necessary in the above model. For

sufficiently small, widely-spaced particles, the flows are locally linear and particle interactions are negligible, and Leal and Hinch (1972) have shown that the orientation p.d.f. satisfies a Fokker-Planck equation on the unit sphere,

$$\frac{\partial f}{\partial t} + \nabla \cdot (\dot{\boldsymbol{p}} f) = D_r \nabla^2 f \,, \tag{1}$$

where the torque balance, from Leal and Hinch (1972) and Hinch and Leal (1972) (but initially derived by Jeffrey 1922), is written as

$$\dot{\boldsymbol{p}} = \frac{1}{2B} [\boldsymbol{k} - (\boldsymbol{k} \cdot \boldsymbol{p})\boldsymbol{p}] + \frac{1}{2} \boldsymbol{\Omega} \wedge \boldsymbol{p} + \alpha_0 \boldsymbol{p} \cdot \boldsymbol{E} \cdot (\boldsymbol{I} - \boldsymbol{pp}) \,. \tag{2}$$

Here, ∇ is the gradient operator in $\boldsymbol{p}$-space, α_0 is the particle eccentricity, B is a reorientation time scale, balancing external and viscous torques, $\boldsymbol{k}$ is a vertical unit vector, $\boldsymbol{\Omega}$ is the local fluid vorticity and $\boldsymbol{E}$ is the local rate-of-strain tensor. We can neglect the $\partial f/\partial t$ term in (1) if we can also assume that the time scales for variations in the flow are much longer than the particle orientation times, D_r^{-1} and B, so that the particle distribution has sufficient time to equilibriate to a quasi-steady state. The particle eccentricity is important when considering straining flows. For the case where $\alpha_0 = 0$, the particle is spherical and is not affected by straining motion in the fluid. The first term on the right hand side of (2) represents the gravitational torque due to the asymmetric mass distribution (Pedley and Kessler 1992) but could also represent any external mechanical torque on dipolar particles within an external field (Brenner and Weissman 1972). An application that uses similar expressions is also found in flow visualization using reflective flakes (see Savas 1985).

$\boldsymbol{\Omega}$ and $\boldsymbol{E}$ are non-dimensionalised with respect to a typical vorticity scale, Ω, such that $\boldsymbol{\omega} = \boldsymbol{\Omega}/\Omega$ and $\boldsymbol{e} = \boldsymbol{E}/\Omega$, and, after some algebra (Pedley and Kessler 1990), Equations (1) and (2) give

$$\boldsymbol{k} \cdot \nabla f - 2(\boldsymbol{k} \cdot \boldsymbol{p}) f + \eta \boldsymbol{\omega} \cdot (\boldsymbol{p} \wedge \nabla f) + 2\eta\alpha_0 [\boldsymbol{p} \cdot \boldsymbol{e} \cdot \nabla f - 3\boldsymbol{p} \cdot \boldsymbol{e} \cdot \boldsymbol{p} f] = \lambda^{-1} \nabla^2 f \tag{3}$$

where[1]

$$\lambda = \frac{1}{2D_r B} \quad \text{and} \quad \eta = B\boldsymbol{\Omega} \,. \tag{4}$$

Hill et al. (1989) calculated λ for *C. nivalis* to be approximately equal to 2.2 from measurements of cell diffusivities.

Bioconvection occurs as a result of the passive or active orientation mechanisms of many microscopic swimming individuals and is realised as the

[1]Note: λ differs by a factor of $\frac{1}{2}$ omitted in error in Pedley and Kessler (1990) but corrected in Pedley and Kessler (1992).

bulk motion of a suspension of such individuals on much larger scales than the dimensions of the micro-organisms (Platt 1961; Childress et al. 1975; Kessler 1986; Pedley and Kessler 1992; Bees and Hill 1997a), resulting in patterns reminiscent of thermal convection. Therefore, it requires modelling at both microscopic and macroscopic scales to understand the system fully. The micro-organisms in question are bottom heavy and, hence, negatively gravitactic in that on average they swim upwards. However, if they are denser than the ambient fluid then aggregations of the cells at an upper boundary can cause overturning. Additionally, another mechanism for instability that does not require an upper boundary is often observed in cultures of some micro-organisms (such as the alga *Chlamydomonas nivalis*). The mechanism is termed gyrotaxis, after Kessler (1984), and is caused by viscous torques acting on the individual cells, thus influencing their average swimming directions. A region of downwelling flow can tip cells' axes away from the vertical so that they swim towards the centre of the downwelling region. An instability is generated if the cells are denser than the surrounding fluid, thus causing the sinking fluid to sink even faster and attract even more cells.

In a general fluid the cells have a mean swimming direction, given by the ensemble average of the orientation vector, $\langle \boldsymbol{p} \rangle$, and their stochastic behaviour can be modelled using a tensorial diffusivity, $\boldsymbol{D}$. Both these quantities are functions of space and time. The cell flux due to swimming, $\boldsymbol{J}_s$, is given by

$$\boldsymbol{J}_s = nV_s\langle \boldsymbol{p} \rangle - \boldsymbol{D} \cdot \nabla n \tag{5}$$

where $n = n(x, t)$ is the cell concentration and V_s is the mean cell swimming speed. Higher moments of the orientational p.d.f. are used to calculate $\boldsymbol{D}$ as will be discussed in Sect. 3. Earlier models of bioconvection made an ad hoc approximation for the diffusivity due to the variations in the micro-organisms' swimming but Pedley and Kessler (1990) demonstrated the importance of a more rational approach. They showed that the probability density function, $f(\boldsymbol{p})$, for a gyrotactic micro-organism with swimming direction $\boldsymbol{p}$, satisfies a steady Fokker-Planck equation, given by (3), where $B = \mu\alpha_\perp/2h\rho g$ is now interpreted as the gyrotactic orientation parameter, μ is the fluid viscosity, h is the centre of mass offset from the geometrical centre, ρ is the density of the cells, g is the acceleration due to gravity and $\alpha_\perp$ is the dimensionless resistance coefficient for rotation about an axis perpendicular to $\boldsymbol{p}$ (Pedley and Kessler 1990, Appendix A). Brenner and Weissman (1972) studied a similar form of equation when investigating the rheology of a dilute suspension of dipolar spherical particles in an external field. They obtained good results by expanding in terms of spherical harmonics and using numerical techniques to solve a truncated set of equations for the coefficients. Strand and Kim (1992) have used spherical harmonic expansions for dipolar non-spherical particles in an external field. The authors of both papers used their solutions to investigate the rheological properties of suspensions of particles.

We also adopt this approach but employ the powerful tools of computer algebra. This enables us to solve the truncated set of simultaneous equations

for the coefficients of the spherical harmonics exactly, thus obtaining analytical approximations. Moreover, we derive expressions for the moments of the particle orientation and, hence, the mean cell swimming direction and cell diffusivity tensor, used in models of bioconvection, without further approximation. In many ways, spherical harmonics are the natural eigenfunctions to use in such an expansion, exemplified by the compact expressions for the above two quantities. Only the first five coefficients in the spherical harmonic expansion are required (Bees 1996). The manageable expressions obtained from this work have been applied to non-linear studies of bioconvection which will be presented in another paper (Bees and Hill 1997b).

In this paper, particles are suspended in a fluid whose flow is restricted to being two-dimensional in a vertical plane so that the vorticity vector is horizontal, although in Sect. 4 it is shown that a three-dimensional flow with no vertical component of vorticity can be reduced to essentially the same form. It is still essential to model the particle orientation on a full sphere rather than on a circle as there is a non-zero probability of particles orientated in a direction out of the plane of flow. A spherical polar coordinate system (r, θ, ϕ), is used together with an expansion in terms of $\cos m\phi\, P_n^m(\cos\theta)$ where $P_n^m(x)$ are associated Legendre polynomials. By recursively applying a set of identities for spherical harmonics, using the computer algebra package Maple and truncating at order R, a set of $R(R+3)/2$ equations in as many unknowns is generated, together with a normalisation condition. Maple is again employed to solve this set of equations using exact arithmetic (see Appendix C of Bees 1996 for the Maple code).

2 Expansion in spherical harmonics for two-dimensional flows

The orientation of particles is specified using a spherical polar coordinate system on a unit sphere. The azimuthal angle, θ, and meridonal angle, ϕ, are chosen such that the non-dimensional vorticity, given by $\boldsymbol{\omega} = \omega \boldsymbol{j}$, is perpendicular to the plane in which $\phi = 0$ and $\theta = 0$ indicates an upwards pointing particle (Fig. 1). The particle orientation, $\boldsymbol{p}$, and unit vectors $\hat{\boldsymbol{\phi}}$ and $\hat{\boldsymbol{\theta}}$ are given in terms of Cartesian axes $\boldsymbol{i}, \boldsymbol{j}$ and $\boldsymbol{k}$, where $\boldsymbol{k}$ is vertical, by

$$\boldsymbol{p} = \begin{pmatrix} \sin\theta\cos\phi \\ \sin\theta\sin\phi \\ \cos\theta \end{pmatrix}, \quad \hat{\boldsymbol{\theta}} = \begin{pmatrix} \cos\theta\cos\phi \\ \cos\theta\sin\phi \\ -\sin\theta \end{pmatrix} \quad \text{and} \quad \hat{\boldsymbol{\phi}} = \begin{pmatrix} -\sin\phi \\ \cos\phi \\ 0 \end{pmatrix}. \tag{6}$$

Hence,

$$\begin{aligned} \boldsymbol{\omega}\cdot\boldsymbol{p}\wedge\hat{\boldsymbol{\theta}} &= \omega\cos\phi \\ \boldsymbol{\omega}\cdot\boldsymbol{p}\wedge\hat{\boldsymbol{\phi}} &= -\omega\cos\theta\sin\phi\ . \end{aligned} \tag{7}$$

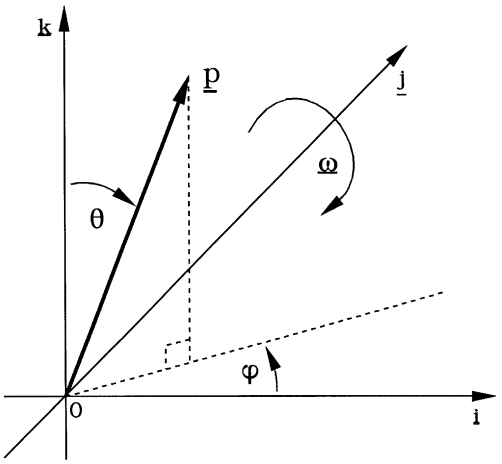

Fig. 1. The choice of coordinate system on a sphere

The non-dimensional rate-of-strain tensor, $\boldsymbol{e}$, can be written as

$$\boldsymbol{e} = \begin{pmatrix} e_{11} & 0 & e_{13} \\ 0 & 0 & 0 \\ e_{13} & 0 & -e_{11} \end{pmatrix} \tag{8}$$

and then

$$\begin{aligned} \boldsymbol{p}\cdot\boldsymbol{e}\cdot\boldsymbol{p} &= e_{11}[\tfrac{1}{4}(\cos 2\phi + 3)(1 - \cos 2\theta) - 1] + e_{13}\sin 2\theta\cos\phi \\ \boldsymbol{p}\cdot\boldsymbol{e}\cdot\hat{\boldsymbol{\theta}} &= e_{11}[\tfrac{1}{4}(\cos 2\phi + 3)\sin 2\theta] + e_{13}\cos 2\theta\cos\phi \\ \boldsymbol{p}\cdot\boldsymbol{e}\cdot\hat{\boldsymbol{\phi}} &= e_{11}[-\tfrac{1}{2}\sin 2\phi\sin\theta] - e_{13}\cos\theta\sin\phi\ . \end{aligned} \tag{9}$$

Hence, the Fokker-Planck Equation (3) becomes

$$\begin{aligned} &\frac{\lambda^{-1}}{\sin\theta}\partial_\theta(\sin\theta\partial_\theta f) + \frac{\lambda^{-1}}{\sin^2\theta}\partial_\phi^2 f + \sin\theta\partial_\theta f + 2\cos\theta f \\ &= \eta\left(\omega\cos\phi\partial_\theta f - \omega\frac{\cos\theta}{\sin\theta}\sin\phi\partial_\phi f\right) \\ &\quad + 2\alpha_0\eta\Bigg[(e_{11}(\cos^2\phi + 1)\sin\theta\cos\theta + e_{13}(\cos^2\theta - \sin^2\theta)\cos\phi)\partial_\theta f \\ &\quad - \left(e_{11}\cos\phi\sin\phi + e_{13}\sin\phi\frac{\cos\theta}{\sin\theta}\right)\partial_\phi f \\ &\quad - 3\left(e_{11}(\sin^2\theta\cos^2\phi - \cos^2\theta) + 2e_{13}\sin\theta\cos\theta\cos\phi\right)f\Bigg]. \end{aligned} \tag{10}$$

For a two dimensional flow, the particle orientation p.d.f. will be symmetric about the flow plane and only even spherical harmonics in ϕ are needed. Expanding f in spherical harmonics gives

$$f = \sum_{n=0}^{\infty} \sum_{m=0}^{n} F_n^m \tag{11}$$

where we define for ease of writing

$$F_n^m(\theta, \phi) \equiv R_n^m(\phi) P_n^m(\cos\theta) \equiv A_n^m \cos m\phi P_n^m(x) \equiv A_n^m Q_n^m(\theta, \phi) . \tag{12}$$

Here $x \equiv \cos\theta$, the coefficients A_n^m depend on the flow field and P_n^m are associated Legendre polynomials (Arfken 1985).

Substituting this series into Equation (10), gives

$$\begin{aligned}
&\sum_{m,n} \{\lambda^{-1} F_n^m[-n(n+1)] - R_n^m P_n^{m\prime} \sin^2\theta + 2\cos\theta F_n^m\} \\
&= \sum_{m,n} \Big\{ -\eta(\omega \cos\phi \sin\theta R_n^m P_n^{m\prime} + \omega \cot\theta \sin\phi R_n^{m\prime} P_n^m) \\
&\quad - 2\alpha_0 \eta \Big[(e_{11}(\cos^2\phi + 1)\sin^2\theta \cos\theta \\
&\quad + e_{13}(\cos^2\theta - \sin^2\theta)\cos\phi \sin\theta) R_n^m P_n^{m\prime} \\
&\quad + (e_{11}\cos\phi \sin\phi + e_{13}\sin\phi \cot\theta) R_n^{m\prime} P_n^m \\
&\quad + 3(e_{11}(\sin^2\theta \cos^2\phi - \cos^2\theta) + 2e_{13}\sin\theta \cos\theta \cos\phi) R_n^m P_n^m \Big] \Big\}
\end{aligned} \tag{13}$$

where a prime denotes differentiation with respect to the dependent variable.

The normalisation condition that f integrates to one over the surface of the sphere implies that

$$A_0^0 = \frac{1}{4\pi} . \tag{14}$$

3 Calculating the moments

Here we shall derive exact expressions for the first and second moments of $\boldsymbol{p}$ (Mardia 1972) and describe an application directly relevant to bioconvection. Firstly, consider the mean orientation $\langle \boldsymbol{p} \rangle$. If S represents the surface of a unit sphere then

$$\langle \boldsymbol{p} \rangle = \int_S \begin{pmatrix} \sin\theta\cos\phi \\ \sin\theta\sin\phi \\ \cos\theta \end{pmatrix} f(\theta, \phi)\, dS \equiv \int_S \begin{pmatrix} Q_1^1 \\ 0 \\ Q_1^0 \end{pmatrix} f(\theta, \phi)\, dS \tag{15}$$

and thus we require the integrals of $\int_S Q_1^1 f dS$ and $\int_S Q_1^0 f dS$. Using Equation (11) and the identities

$$\int_S Q_n^m Q_{n'}^{m'} dS = \delta_{m'}^m \delta_{n'}^n \frac{2\pi}{2n+1} \frac{(n+m)!}{(n-m)!} \tag{16}$$

for $n, n' \geqq m, m' = 1, 2, \ldots$ and

$$\int_S Q_n^0 Q_{n'}^{m'} dS = \delta_{m'}^0 \delta_{n'}^n \frac{4\pi}{2n+1}, \tag{17}$$

we find that

$$\langle \boldsymbol{p} \rangle = \frac{4\pi}{3} \begin{pmatrix} A_1^1 \\ 0 \\ A_1^0 \end{pmatrix}. \tag{18}$$

Similarly, using the identities

$$\sin^2\theta \cos^2\phi = \tfrac{1}{2}\sin^2\theta(1 + \cos 2\phi) = \tfrac{1}{3}Q_0^0 - \tfrac{1}{3}Q_2^0 + \tfrac{1}{6}Q_2^2, \tag{19}$$

$$\sin\theta \cos\theta \cos\phi = \tfrac{1}{3}Q_2^1, \tag{20}$$

$$\cos^2\theta = \tfrac{2}{3}Q_2^0 + \tfrac{1}{3}Q_0^0 \tag{21}$$

and

$$\sin^2\theta \sin^2\phi = \tfrac{1}{2}\sin^2\theta(1 + \cos 2\phi) = \tfrac{1}{3}Q_0^0 - \tfrac{1}{3}Q_2^0 - \tfrac{1}{6}Q_2^2 \tag{22}$$

gives the second moment as

$$\langle \boldsymbol{pp} \rangle = \pi \begin{pmatrix} \frac{4}{3}A_0^0 - \frac{4}{15}A_2^0 + \frac{8}{5}A_2^2 & 0 & \frac{4}{5}A_2^1 \\ 0 & \frac{4}{3}A_0^0 - \frac{4}{15}A_2^0 - \frac{8}{5}A_2^2 & 0 \\ \frac{4}{5}A_2^1 & 0 & \frac{8}{15}A_2^0 + \frac{4}{3}A_0^0 \end{pmatrix}. \tag{23}$$

An application of these expressions arises in the modelling of bioconvection. If $f(\boldsymbol{p})$ is taken to be the p.d.f. for a cell orientation of $\boldsymbol{p}$ then $\langle \boldsymbol{p} \rangle$ represents the mean cell swimming direction (although it is not a unit vector).

Another quantity of interest is the spread of cell orientations at a point in the flow and hence the spread of possible trajectories. The cell diffusion tensor is defined as

$$\boldsymbol{D}(t) = \int_0^\infty \langle \boldsymbol{V}_r(t) \boldsymbol{V}_r(t - t') \rangle \, dt', \tag{24}$$

where $\boldsymbol{V}_r$ is the velocity of a cell relative to its mean value. The expression for $\boldsymbol{D}$ is, of course, hard to calculate as it requires a knowledge of all previous cell velocities and, hence, we are forced to make an approximation for the sake of simplicity. Following Pedley and Kessler (1990), we assume that it takes a cell τ seconds to settle to a preferred direction (the direction correlation time).

τ may vary slightly with other parameters, such as η or λ, but in this paper we assume that it is constant and concentrate on the tensorial structure of $\boldsymbol{D}$. Hence,

$$\boldsymbol{D} = \tau(\langle \boldsymbol{V}\boldsymbol{V} \rangle - \langle \boldsymbol{V} \rangle^2) = \tau(\lambda, \eta)\mathrm{Var}(\boldsymbol{V}) \,, \tag{25}$$

where $\boldsymbol{V}$ is the cell swimming velocity. Assuming that the swimming speed, V, and swimming direction, $\boldsymbol{p}$, are independent random variables, we can write $\boldsymbol{V} = V\boldsymbol{p}$. If the mean cell swimming speed $\langle V \rangle = V_s$, then

$$\boldsymbol{D} = V_s^2 \tau(\lambda, \eta)\left(\frac{\langle V^2 \rangle}{V_s^2}\langle \boldsymbol{p}\boldsymbol{p} \rangle - \langle \boldsymbol{p} \rangle^2\right). \tag{26}$$

Varying the ratio

$$\mathcal{N} = \frac{\langle V^2 \rangle}{V_s^2} \tag{27}$$

changes the nature of the diffusion tensor. The data of Hill and Häder (1997) give $\mathcal{N}$ as bounded by 1.15 and 1.45 for the swimming, single-celled alga *C. nivalis*. Substituting for the moments of $\boldsymbol{p}$ from Equations (18) and (23) yields

$$\frac{\boldsymbol{D}}{\mathcal{N} V_s^2 \tau \pi} = \begin{pmatrix} \frac{4}{3}A_0^0 - \frac{4}{15}A_2^0 + \frac{8}{5}A_2^2 - \frac{16\pi}{9\mathcal{N}}(A_1^1)^2 & 0 & \frac{4}{5}A_2^1 - \frac{16\pi}{9\mathcal{N}}A_1^1 A_1^0 \\ 0 & \frac{4}{3}A_0^0 - \frac{4}{15}A_2^0 - \frac{8}{5}A_2^2 & 0 \\ \frac{4}{5}A_2^1 - \frac{16\pi}{9\mathcal{N}}A_1^1 A_1^0 & 0 & \frac{8}{15}A_2^0 + \frac{4}{3}A_0^0 - \frac{16\pi}{9\mathcal{N}}(A_1^0)^2 \end{pmatrix}. \tag{28}$$

Thus the only expressions required are those for the five coefficients A_1^0, A_1^1, A_2^0, A_2^1 and A_2^2 in the spherical harmonic expansion.

4 Three-dimensional flows

In some circumstances, for example when the observed bioconvection patterns possess particular symmetries, it may be reasonable to assume that there is no component of vorticity in the vertical direction. If we also assume that $\alpha_0 = 0$ so that the rate-of-strain in the fluid does not affect the particle orientation then we can construct an approximation to the diffusion tensor, similar to the above, for use in three-dimensional applications. In particular, the flow field, $\boldsymbol{u}$, can be written in terms of a poloidal velocity field, F, such that

$$\boldsymbol{u} = \nabla \wedge \nabla \wedge (F\boldsymbol{k}) \,. \tag{29}$$

Locally we rotate the "plane of solution" about a vertical axis, so that $\boldsymbol{\omega}$ is always perpendicular to the plane $\phi = 0$. The Fokker-Planck equation can be expanded in terms of surface spherical harmonics, as before, and can then be

rotated back to the original coordinate system in the integral definitions of $\langle \boldsymbol{p} \rangle$ and $\boldsymbol{D}$.

We define the angle of rotation, ψ, to be

$$\psi = \arctan\left(\frac{\omega_1}{\omega_2}\right), \tag{30}$$

where

$$\boldsymbol{\omega} = \begin{pmatrix} \omega_1 \\ \omega_2 \\ 0 \end{pmatrix} \tag{31}$$

and put $\omega^2 = \omega_1^2 + \omega_2^2$. Then

$$\langle \boldsymbol{p} \rangle = \int_S f(\theta, \phi - \psi)\boldsymbol{p}\, dS\,, \tag{32}$$

where f is evaluated in the rotated frame. Putting $\bar{\phi} = \phi - \psi$ then

$$\langle \boldsymbol{p} \rangle = \int_S f(\theta, \bar{\phi}) \begin{pmatrix} \sin\theta\cos(\bar{\phi} + \psi) \\ \sin\theta\sin(\bar{\phi} + \psi) \\ \cos\theta \end{pmatrix} dS\,. \tag{33}$$

The trigonometric functions $\cos(\bar{\phi} + \psi)$ and $\sin(\bar{\phi} + \psi)$ in (33) can be expanded and hence

$$\langle \boldsymbol{p} \rangle = \int_S f(\theta, \bar{\phi}) \begin{pmatrix} Q_1^1 \cos\psi \\ Q_1^1 \sin\psi \\ Q_1^0 \end{pmatrix} dS\,, \tag{34}$$

which, when f is written as a sum of spherical harmonics as in Sect. 3, implies that

$$\langle \boldsymbol{p} \rangle = \frac{4}{3}\pi \begin{pmatrix} A_1^1 \cos\psi \\ A_1^1 \sin\psi \\ A_1^0 \end{pmatrix} \tag{35}$$

in the original coordinates. In a similar way

$$\langle \boldsymbol{pp} \rangle = \int_S f(\theta, \bar{\phi})\boldsymbol{M}\, dS \tag{36}$$

where $\boldsymbol{M}$ is equal to

$$\begin{pmatrix} \sin^2\theta\cos^2(\bar{\phi} + \psi) & \sin^2\theta\cos(\bar{\phi} + \psi)\sin(\bar{\phi} + \psi) & \cos\theta\sin\theta\cos(\bar{\phi} + \psi) \\ \sin^2\theta\cos(\bar{\phi} + \psi)\sin(\bar{\phi} + \psi) & \sin^2\theta\sin^2(\bar{\phi} + \psi) & \cos\theta\sin\theta\sin(\bar{\phi} + \psi) \\ \cos\theta\sin\theta\cos(\bar{\phi} + \psi) & \cos\theta\sin\theta\sin(\bar{\phi} + \psi) & \cos^2\theta \end{pmatrix}. \tag{37}$$

Substituting the surface spherical harmonics for f, expanding and evaluating, gives

$$\langle \boldsymbol{pp} \rangle = \pi \begin{pmatrix} \frac{4}{3}A_0^0 - \frac{4}{15}A_2^0 + \frac{8}{5}A_2^2\cos 2\psi & \frac{8}{5}A_2^2 \sin 2\psi & \frac{4}{5}A_2^1\cos\psi \\ \frac{8}{5}A_2^2\sin 2\psi & \frac{4}{3}A_0^0 - \frac{4}{15}A_2^0 - \frac{8}{5}A_2^2\cos 2\psi & \frac{4}{5}A_2^1\sin\psi \\ \frac{4}{5}A_2^1\cos\psi & \frac{4}{5}A_2^1\sin\psi & \frac{8}{15}A_2^0 + \frac{4}{3}A_0^0 \end{pmatrix}. \tag{38}$$

The A's are all functions of $\omega = \sqrt{\omega_1^2 + \omega_2^2}$ and by using $\tan\psi = \omega_1/\omega_2$ we can write $\cos\psi = \omega_1/\omega$, $\sin\psi = \omega_2/\omega$, $\cos 2\psi = \omega_2^2 - \omega_1^2/\omega^2$ and $\sin 2\psi = 2\omega_1\omega_2/\omega^2$. As before, these expressions can be used to calculate $\mathrm{Var}(\boldsymbol{V})$ and, hence, $\boldsymbol{D}$ in Equation (26).

5 Simplification

The expansion of the Fokker-Planck Equation (13) is split into three parts. $\mathscr{G}_n^m$ will be used to signify the summand for intermediate values of m, and $\mathscr{F}_n^0$ and $\mathscr{F}_n^1$ will be used to signify the summands for the special cases when $m = 0$ and 1. Thus the complete expansion of Equation (13) can be written as

$$\sum_{n=0}^{R} \mathscr{F}_n^0 + \sum_{n=1}^{R} \mathscr{F}_n^1 + \sum_{n=2}^{R} \sum_{m=2}^{n} \mathscr{G}_n^m = 0\,, \tag{39}$$

where R is the order of the approximation and the spherical harmonic coefficients, A_q^p (see Equation (12)), are zero if $p > q$, $p < 0$, $q > R$ or $q < 0$.

We consider Equation (13) one term at a time, trying at each stage to express the relevant term as an expression which is linear in Q_n^m with simple non-trigonometric coefficients. The operators and identities listed in the Appendix will be employed. Henceforth, we set $x \equiv \cos\theta$ and make use of the shorthand $S^m \equiv \sin m\phi$ and $C^m \equiv \cos m\phi$.

5.1 Left-hand side

The first term on the left hand side of (13) is in the correct form. Applying the operator X_{ssp} (defined in the Appendix) to the second term, gives terms involving $Q_{n\pm1}^m$. Similarly applying X_c to the third term gives terms involving $Q_{n\pm1}^m$.

5.2 Right-hand side: vorticity terms

The first term on the right hand side contains C^1 so we make use of the identity X_{cos} and turn the R_n^m into $A_n^m(C^{m-1} + C^{m+1})/2$. Now we convert the

$P_n^{m\prime}$ terms into terms like $P_n^{m\pm1}$. This proves possible with the identities X_{spu} and X_{spd}. However, there appears to be an undesirable term, $\pm P_n^m mx/\sqrt{1-x^2}$. If this term were to remain in the equation, then it would lead to the problematic integral

$$\int \frac{1}{1-x^2} P_n^m(x)\, P_p^m(x)\, dx \tag{40}$$

which, on explicit evaluation, gives not one delta function in terms of n and p, but an infinite series of delta functions in n and p since

$$\int \frac{1}{1-x^2} P_n^m(x) P_p^m(x)\, dx = \begin{cases} \dfrac{1}{m}\dfrac{(\min(p,n)+m)!}{(\min(p,n)-m)!} & p+n \text{ even} \\ 0 & \text{otherwise .} \end{cases} \tag{41}$$

The integral is unusual in that only $\min(p, n)$ is relevant and not $\max(p, n)$ (Appendix B, Bees 1996). This procedure would ultimately give an infinite set of infinite-length recursion relations for the A_n^m. However, these terms completely cancel out with similar terms produced by the second term on the right hand side, after application of the identity $X_{\sin}$. Thus, the vorticity terms become

$$\frac{\omega\eta A_n^m}{2}(-Q_n^{m+1} + (n-m+1)\,(n+m)\,Q_n^{m-1}) . \tag{42}$$

5.3 *Right-hand side: rate-of-strain terms*

These terms naturally fall into two groups: the third, fifth and seventh terms multiplied by e_{11}, and the fourth, sixth and eighth terms multiplied by e_{13}. Using the identities $X_{\cos}$ and $X_{\sin}$, the terms in the first group can be written in terms of $C^{m\pm2}$ and C^m, with the "undesirable" terms always cancelling.

5.4 *Summand: intermediate terms*

The whole of Equation (13), for intermediate values of m, finally becomes

$$\begin{aligned} \mathscr{G}_n^m := {} & \lambda^{-1} n(n+1) A_n^m Q_n^m + A_n^m X_{ssp}(Q_n^m) - 2A_n^m X_c(Q_n^m) \\ & + \frac{\omega\eta}{2} A_n^m(-Q_n^{m+1} + (n-m+1)\,(n+m) Q_n^{m-1}) \\ & - 2\alpha_0\eta e_{11} A_n^m \Big[-\frac{1}{4}(n-m+1)\,(m+n) X_c(X_{sd}(Q_n^{m-1})) \\ & + \frac{3-m}{4} X_{sd}(X_{sd}(Q_n^m)) + \frac{1}{4} X_c(X_{su}(Q_n^{m+1})) \end{aligned}$$

$$+\frac{3+m}{4}X_{su}(X_{su}(Q_n^m))+\frac{3}{2}X_{ss}(Q_n^m)-3X_c(X_c(Q_n^m))$$

$$+\frac{3}{2}\frac{1}{2n+1}X_c((n+m)(n+1)Q_{n-1}^m-n(n-m+1)Q_{n+1}^m)\Bigg]$$

$$-2\alpha_0\eta e_{13}A_n^m\Bigg[X_c(X_c(-(n-m+1)(n+m)Q_n^{m-1}+Q_n^{m+1}))$$

$$-\frac{1}{2}(-(n-m+1)(n+m)Q_n^{m-1}+Q_n^{m+1})$$

$$-mX_c(X_{sd}(Q_n^m)-X_{su}(Q_n^m))+\frac{3}{2n+1}X_c((n+m)(n+m-1)Q_{n-1}^{m-1}$$

$$-(n-m+1)(n-m+2)Q_{n+1}^{m-1}+Q_{n+1}^{m+1}-Q_{n-1}^{m+1})\Bigg], \tag{43}$$

which will be summed over m and n later.

5.5 *Special cases: extremal terms*

There are two special cases connected with the finite order of the expansion. One concerns the upper extreme of the expansion and the other concerns special cases around the lower extreme. The first is easily dealt with by setting all coefficients of order greater than the truncation order to zero. In the second case, note that $A_n^m=0$ if $m, n<0$ or $n\geqq m$, and such terms should not appear in Equation (43). Consider first the case of $m=0$:

$$S^1S^0=\tfrac{1}{2}C^{-1}-\tfrac{1}{2}C^1=0 \tag{44}$$

and

$$C^1C^0=\tfrac{1}{2}C^{-1}+\tfrac{1}{2}C^1=C^1\,, \tag{45}$$

in which $C^m=\cos m\phi$ and $S^m=\sin m\phi$. These indicate how the definitions (116) and (114) for $X_{\cos}$ and $X_{\sin}$ need to be modified. In general, if $m=0$ then terms in Q_q^p where p is positive are doubled and where p is negative are set to zero. Terms where $p=0$ are unchanged. This gives us the following relations for all values of n, which will be summed over n later:

$$\mathscr{F}_n^0:=\lambda^{-1}n(n+1)A_n^0Q_n^0+A_n^0X_{ssp}(Q_n^0)-2A_n^0X_c(Q_n^0)-\omega\eta A_n^0Q_n^1$$

$$-2\alpha_0\eta e_{11}A_n^m\Bigg[\frac{1}{2}X_c(X_{su}(Q_n^1))+\frac{3}{2}X_{su}(X_{su}(Q_n^0))+\frac{3}{2}X_{ss}(Q_n^0)$$

$$-3X_c(X_c(Q_n^0))+\frac{3}{2}\frac{1}{2n+1}X_c(n(n+1)Q_{n-1}^0-n(n+1)Q_{n+1}^0)\Bigg]$$

$$-2\alpha_0\eta e_{13}A_n^0\Bigg[2X_c(X_c(Q_n^1))-Q_n^1+\frac{6}{2n+1}X_c(Q_{n+1}^1-Q_{n-1}^1)\Bigg]. \tag{46}$$

The next case to consider is $m = 1$. The only terms which may cause concern here are those that involve expressions in Q_n^{m-2}, all of which have coefficient $\alpha_0 \eta e_{11}$. Taking this into account, we obtain

$$\begin{aligned}
\mathscr{F}_n^1 := {} & \lambda^{-1} n(n+1)\, A_n^1 Q_n^1 + A_n^1 X_{ssp}(Q_n^1) - 2A_n^1 X_c(Q_n^1) \\
& + \frac{\omega\eta}{2} A_n^1(-Q_n^2 + n(n+1)Q_n^0) \\
& - 2\alpha_0\eta e_{11} A_n^1 \Bigg[-\frac{1}{4} n(1+n) X_c(X_{su}(Q_n^0)) + \frac{1}{2} X_{ss}(Q_n^1) \\
& + \frac{1}{4} X_c(X_{su}(Q_n^2)) + X_{su}(X_{su}(Q_n^1)) + \frac{3}{2} X_{ss}(Q_n^1) - 3X_c(X_c(Q_n^1)) \\
& + \frac{3}{2}\frac{1}{2n+1} X_c((n+1)^2 Q_{n-1}^1 - n^2 Q_{n+1}^1) \Bigg] \\
& - 2\alpha_0\eta e_{13} A_n^1 \Bigg[X_c(X_c(-n(n+1)\, Q_n^0 + Q_n^2)) \\
& - \frac{1}{2}(-n(n+1)Q_n^0 + Q_n^2) - X_c(X_{sd}(Q_n^1) - X_{su}(Q_n^1)) \\
& + \frac{3}{2n+1} X_c(n(n+1)Q_{n-1}^0 - n(n+1)Q_{n+1}^0 \\
& + Q_{n+1}^2 - Q_{n-1}^2) \Bigg] . \qquad (47)
\end{aligned}$$

6 Implementation

As the surface spherical harmonics form an orthonormal basis, we can find the inner product of Equation (39) with any other surface spherical harmonic and hence extract a set of $R(R+3)/2$ simultaneous equations for the $R(R+3)/2$ unknown coefficients. The implementation in Maple is straightforward (see Appendix C of Bees (1996) for the Maple code). There are a number of input parameters in the problem. The search of parameter space has been limited by assuming that λ (Equation (4)) is given: for the micro-organism *C. nivalis* $\lambda \approx 2.2$ and this value will be used throughout the following analysis. Furthermore, writing $\lambda = 22/10$ allows Maple to function using integer arithmetic and so avoids truncation errors that can result from many operations of floating point arithmetic. The shorthand

$$\zeta = \eta\omega \,, \qquad (48)$$

$$\xi = \alpha_0 \eta e_{11} \qquad (49)$$

and

$$\chi = \alpha_0 \eta e_{13} \qquad (50)$$

is also employed.

7 Results for $\alpha_0 = 0$

If we set $\alpha_0 = 0$, so that the particles are spherical and the effects of rate-of-strain vanish, then a particle's orientation is determined by a balance between the gravitational and vorticity driven torques. This case is easy to visualise and one can imagine the deterministic situation in which vorticity increases and the particles' angle to the vertical increases with it. If the vorticity increases too much, then the terms no longer balance and the particle tumbles. We expect to see a similar situation with the stochastic model, with the particles' average swimming angle with the vertical increasing with vorticity. For very high values of vorticity, the cell orientation probability density function is no longer sharply peaked but almost uniform.

The five simultaneous equations for the second order approximation are

$$\begin{aligned}
\frac{20}{33}A_1^0 + \frac{2}{3}\zeta A_1^1 + \frac{4}{15}A_2^0 - \frac{1}{3\pi} &= 0 \\
-\frac{2}{3}\zeta A_1^0 + \frac{20}{33}A_1^1 + \frac{2}{5}A_2^1 &= 0 \\
-\frac{4}{5}A_1^0 + \frac{12}{11}A_2^0 + \frac{6}{5}\zeta A_2^1 &= 0 \\
-\frac{6}{5}A_1^1 - \frac{6}{5}\zeta A_2^0 + \frac{36}{11}A_2^1 + \frac{12}{5}A_2^2 &= 0 \\
-\frac{12}{5}\zeta A_2^1 + \frac{144}{11}A_2^2 &= 0\,.
\end{aligned} \tag{51}$$

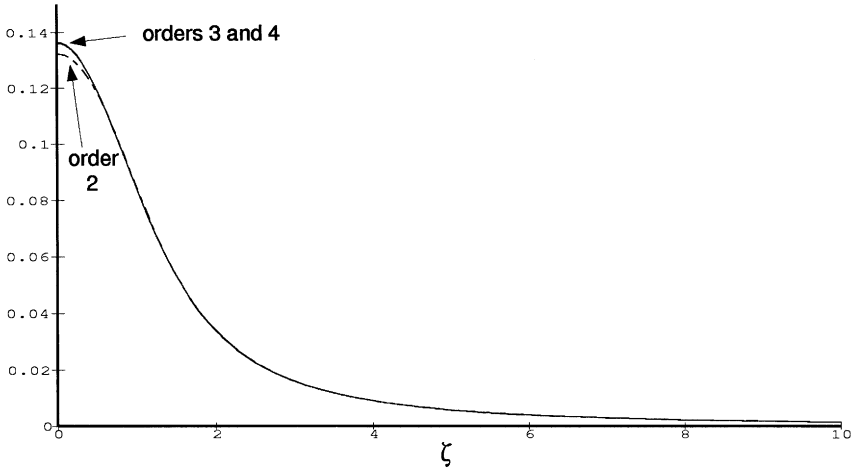

Fig. 2. Graph of the coefficient A_1^0 with ζ for orders of approximation of 2, 3 and 4

This set of equations is remarkably simple. It could be easily extended to the time dependent problem and the resulting linear dynamical system studied. Solving the above equations results in the expressions

$$
\begin{aligned}
A_1^0 &= \frac{825}{4\pi}\,\frac{5589 + 2420\zeta^2}{1098075\zeta^4 + 2363735\zeta^2 + 2772144} \\
A_1^1 &= \frac{1815\zeta}{4\pi}\,\frac{1887 + 1210\zeta^2}{1098075\zeta^4 + 2363735\zeta^2 + 2772144} \\
A_2^0 &= \frac{605}{8\pi}\,\frac{11178 - 4235\zeta^2}{1098075\zeta^4 + 2363735\zeta^2 + 2772144} \\
A_2^1 &= \frac{2495625}{4\pi}\,\frac{\zeta}{1098075\zeta^4 + 2363735\zeta^2 + 2772144} \\
A_2^2 &= \frac{1830125}{16\pi}\,\frac{\zeta^2}{1098075\zeta^4 + 2363735\zeta^2 + 2772144}\,.
\end{aligned}
\tag{52}
$$

These expressions, together with Equations (18) and (28), are used in the non-linear analysis of Bees and Hill (1997b).

Figures 2 and 3 show the graphs of A_1^0 and A_1^1 after truncating at orders 2, 3 and 4. It can be seen that orders 3 and 4 are almost indistinguishable (as are all higher orders) and that even the second order approximation captures the essential behaviour of the system. This is also true for the coefficients A_2^0,

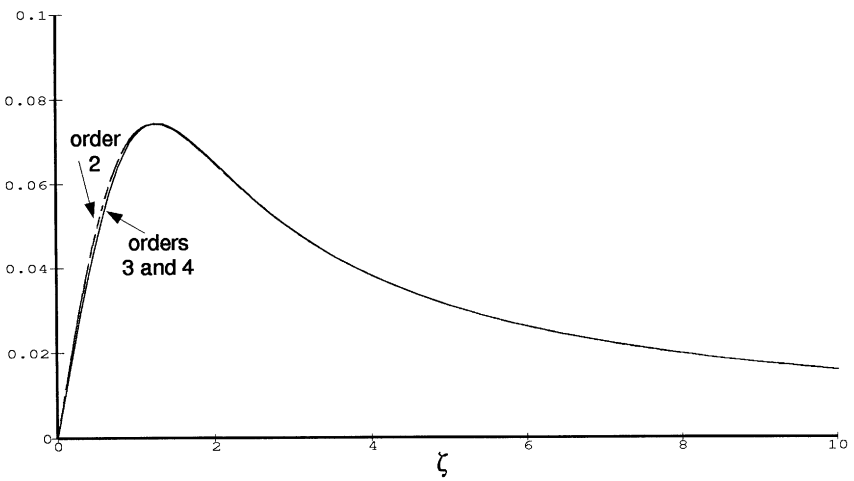

Fig. 3. Graph of the coefficient A_1^1 with ζ for orders of approximation of 2, 3 and 4

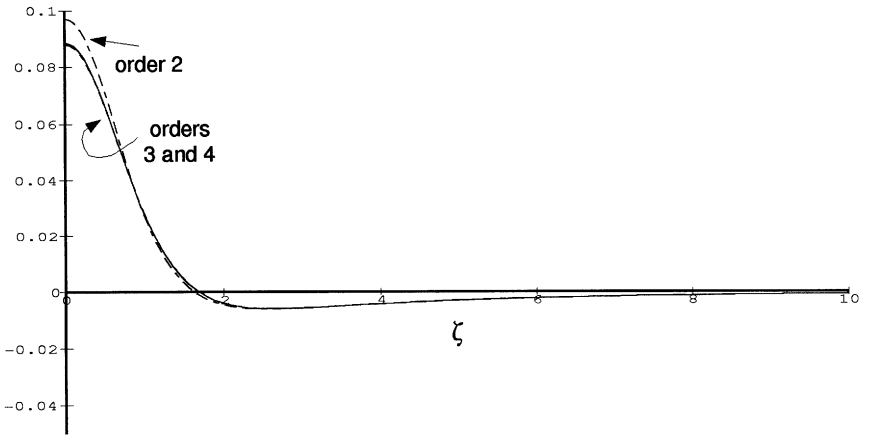

Fig. 4. Graph of the coefficient A_2^0 with ζ for orders of approximation of 2, 3 and 4

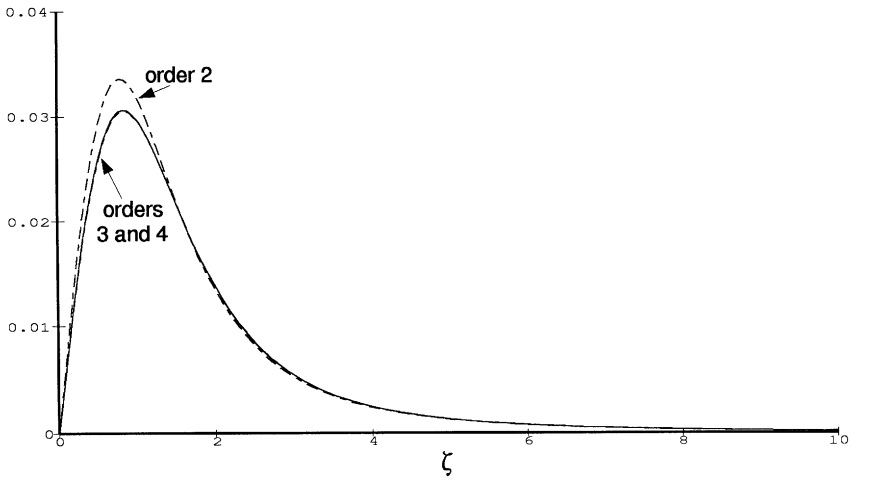

Fig. 5. Graph of the coefficient A_2^1 with ζ for orders of approximation of 2, 3 and 4

A_2^1 and A_2^2 (Figs. 4–6). However, the sizes of the algebraic expressions for the coefficients vary markedly. The expressions quickly become cumbersome and unmanageable after the fourth order. At $\zeta = 0$, the second order approximation for A_1^0 differs by only 3% from the third order approximation.

Section 3 above shows that A_1^1 represents the x component of the particle orientation and A_1^0 the z component. There are no physical mechanisms that result in sharply peaked distributions which may cause resolution problems for $\alpha_0 = 0$. This is not typically the case for $\alpha_0 \neq 0$ as described in the next section. Here, we have chosen a typical value of the parameter λ, and in general as λ increases (i.e. either D_r or B decreases) the distribution becomes more sharply peaked.

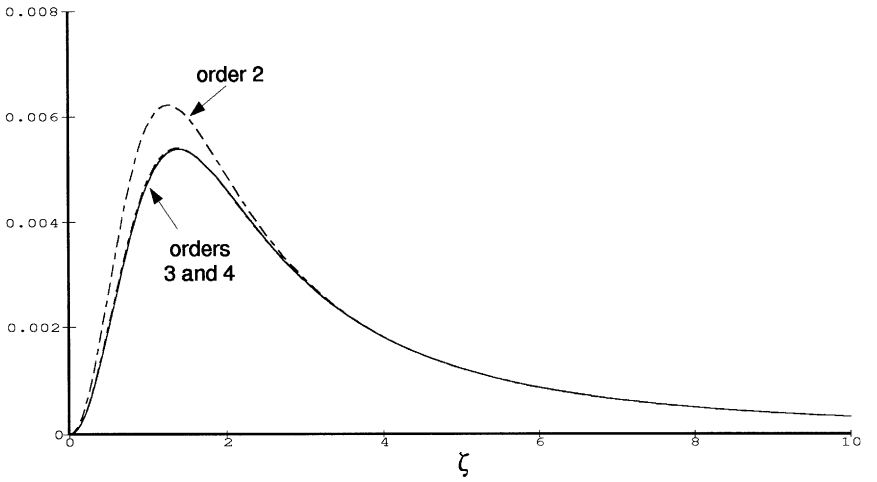

Fig. 6. Graph of the coefficient A_2^2 with ζ for orders of approximation of 2, 3 and 4

8 Results for $\alpha_0 \neq 0$

For an expansion truncated at order R, the coefficients are given by

$$A_n^m = \frac{\mathscr{Y}_n^m[\frac{1}{2}(R+1)^2](\zeta, \xi, \chi)}{\mathscr{Z}[\frac{1}{2}(R+1)^2](\zeta, \xi, \chi)} \tag{53}$$

(by observation) where $\mathscr{Y}_n^m[N](\zeta, \xi, \chi)$ and $\mathscr{Z}[N](\zeta, \xi, \chi)$ denote polynomials in ζ, ξ, and χ, with a maximum combined order of N. We note that $(R+1)^2/2$ is just less than the total number of coefficients, $R(R+3)/2$, as expected, and that the approximation to the particle orientation p.d.f., when χ and $\zeta = 0$, converges rapidly close to $\xi = 0$ (similarly for χ). Otherwise, for low orders of the approximation, spurious singularities arise in the values of the coefficients $A_1^0(\xi)$, $A_1^1(\xi)$, $A_2^0(\xi)$, $A_2^1(\xi)$ and $A_2^2(\xi)$, all of which share the same denominator, $\mathscr{Z}[\frac{1}{2}(R+1)^2](\xi)$. As the order of approximation, R, increases, the singularities move further from the origin. When $R = 10$ the approximation is well behaved in the region $|\xi| \leqq 10$ but singularities still exist in the region $|\xi| \geqq 10$. This behaviour is illustrated in Figs. 7–9. None of the coefficients is a symmetric function of ξ, on account of the very different flow fields, with respect to gravity, for positive or negative e_{11}. Negative values of e_{11} increase the probability that the particle will be orientated vertically, whereas positive values decrease it. The existence of spurious singularities implies that there is a physical difficulty in trying to represent the solutions by a finite sum of spherical harmonics. If e_{11} increases (implying that e_{33} decreases) then the particle orientation becomes more and more likely to be along the x axis and less random. This implies that the distribution becomes more peaked and the number of spherical harmonics may be insufficient to represent it. As the order of approximation increases, the problem is

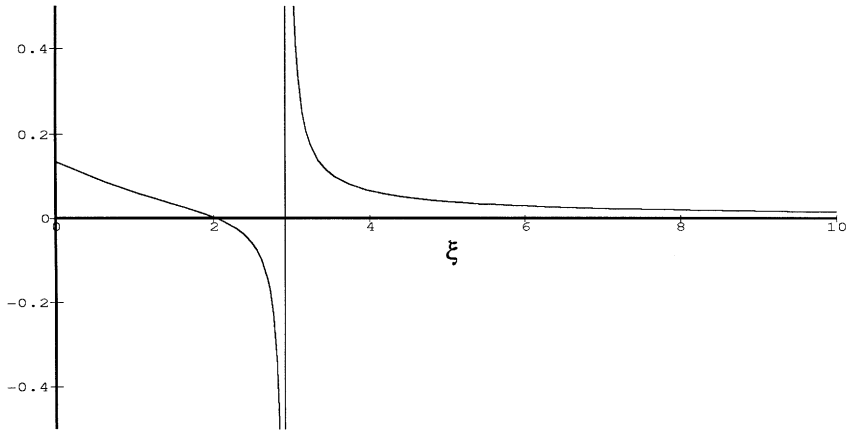

Fig. 7. Graph of the coefficient A_1^0 versus ξ for a third order approximation. $\zeta = \chi = 0$

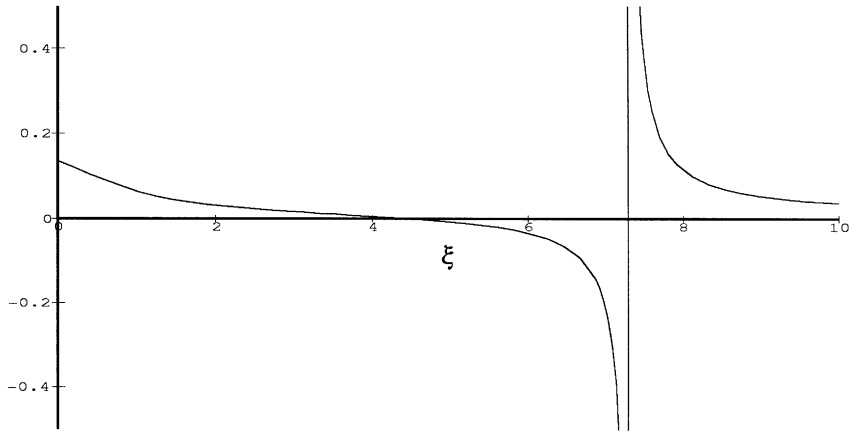

Fig. 8. Graph of the coefficient A_1^0 versus ξ for a seventh order approximation. $\zeta = \chi = 0$

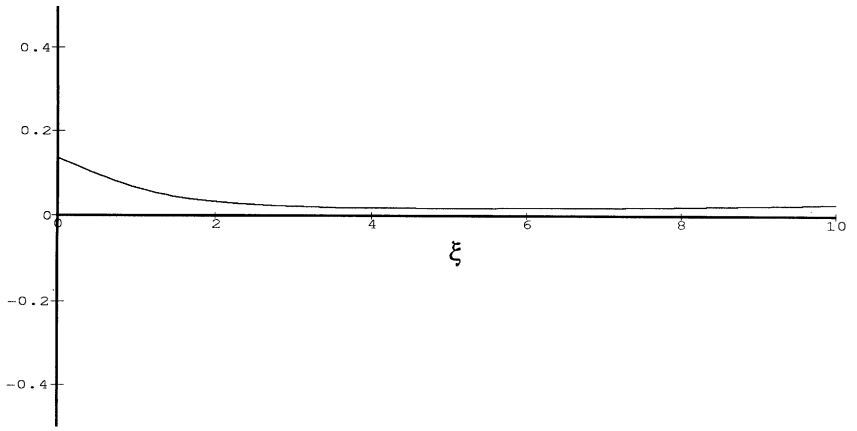

Fig. 9. Graph of the coefficient A_1^0 versus ξ for a tenth order approximation. $\zeta = \chi = 0$

alleviated. However, for $R > 10$ the computer time and space required become excessive, and the Maple expressions become unmanageable.

9 Regions of validity

Figure 10 is a schematic diagram of parameter space. The two regions that exhibit resolution problems are identified and the region where reliable results are obtained is indicated. Although the spherical harmonic approximation for aspherical particles can be discontinuous at all orders of truncation, it does not imply that the method is a failure. The coefficient $A_1^0(\zeta, \xi, \chi)$ actually converges to its true value for reasonably large regions of parameter space. But what are realistic/experimental values for the parameters in bioconvection? Using the definition $\eta = B\Omega$, where Ω is a typical scale for vorticity and rate-of-strain and B is the gyrotaxis orientation parameter, we get

$$\xi \sim \alpha_0 B E_{11} \ , \tag{54}$$

where $E_{11} \sim \Omega$ is a dimensional component of the rate-of-strain tensor. From observations (Childress et al. 1975; Kessler 1985; Bees 1996), a typical fluid velocity will not exceed 1 mm s^{-1} and will change over a distance of 1 mm. This indicates that in experiments $E_{11} \leqq O(1)$. Hence, $\xi \leqq O(1)$ and, in normal situations, the fourth order approximation should be valid.

Figures 11–13 display second order approximations for D_{xx}, D_{xz} and D_{zz}, respectively, versus ζ, when $\xi = \chi = 0$, with different values of $\mathcal{N}$

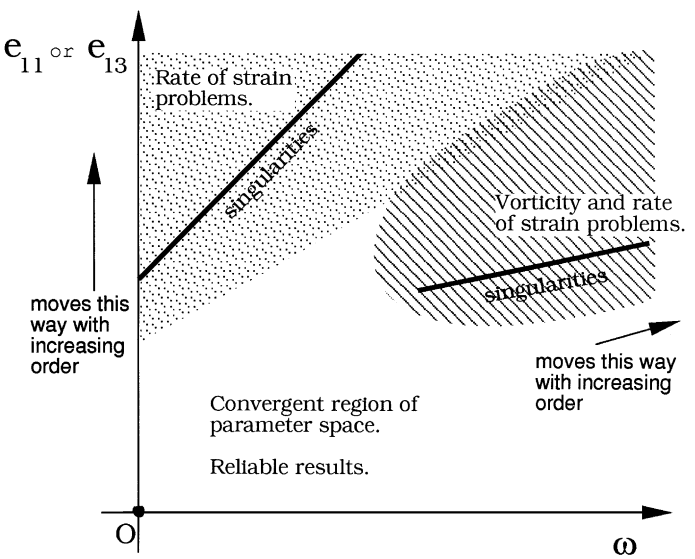

Fig. 10. A schematic diagram of ω and e_{11} space – highlighting the regions of validity when the spherical harmonic approximation is truncated. The solid lines indicate the possibility of spurious singularities and the surrounding shaded regions indicate unreliable results

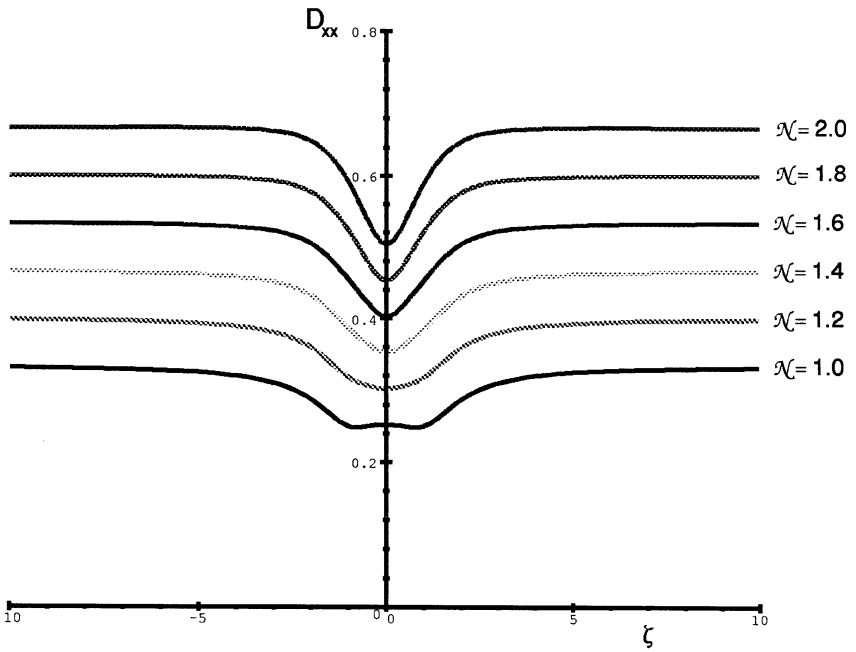

Fig. 11. A graph of D_{xx} with varying ζ and $\mathcal{N}$ for a second order approximation to $f(\theta, \phi)$ with $\alpha_0 = 0$. $\mathcal{N}$ increases with $D_{xx}(0)$ from 1.0 to 2.0

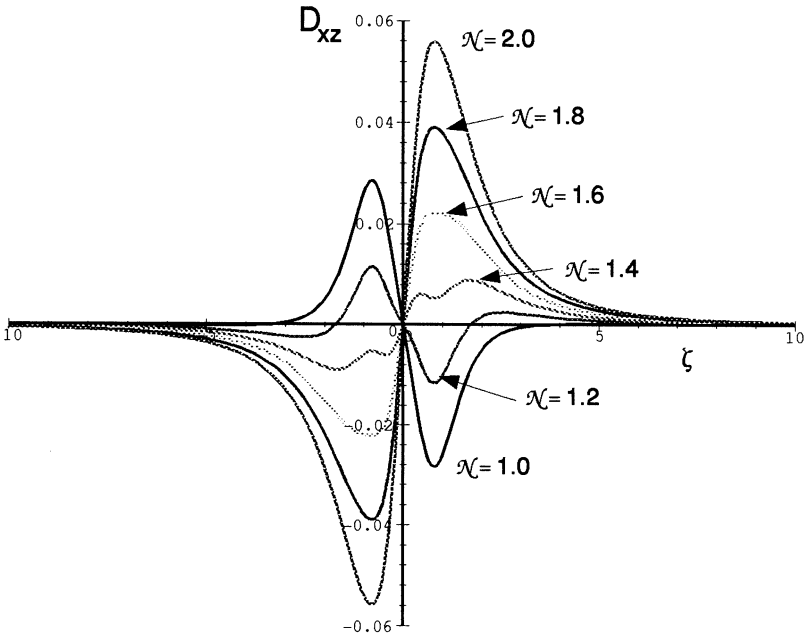

Fig. 12. A graph of D_{xx} with varying ζ and $\mathcal{N}$ for a second order approximation to $f(\theta, \phi)$ with $\alpha_0 = 0$. $\mathcal{N}$ increases with $D_{xx}(0)$ from 1.0 to 2.0

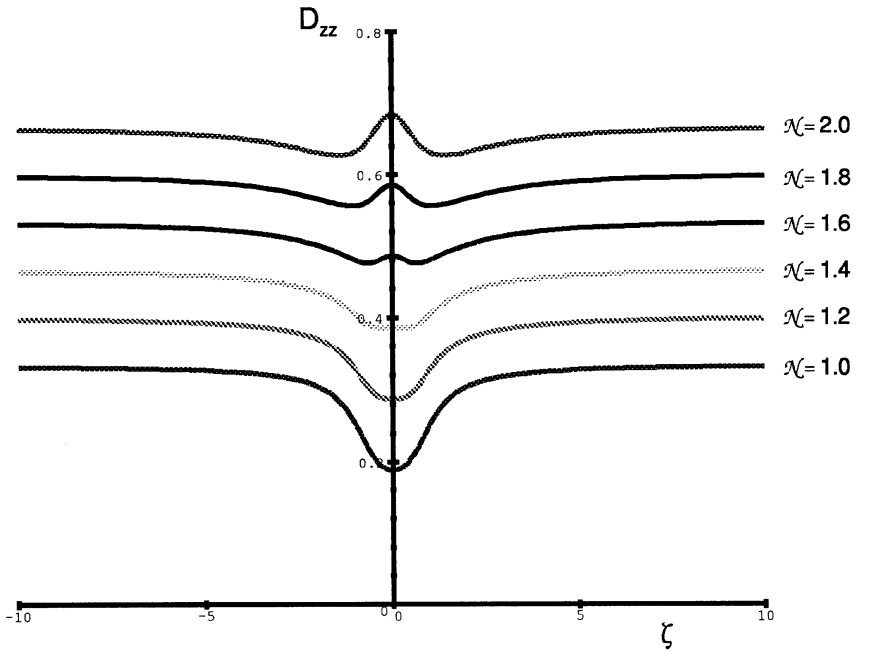

Fig. 13. A graph of D_{xx} with varying ζ and $\mathcal{N}$ for a second order approximation to $f(\theta, \phi)$ with $\alpha_0 = 0$. $\mathcal{N}$ increases with $D_{zz}(0)$ from 1.0 to 2.0

(Equation (27)). Table 1 tabulates D_{xx} and D_{zz} for a selection of ζ and $\mathcal{N}$ and, clearly, the diffusion coefficients quickly converge for increasing truncation order. We see that the diffusion coefficients vary only a small amount and that $D_{xz} \ll D_{xx} \approx D_{zz}$ so that perhaps the assumption of isotropic diffusion made in the earlier models of bioconvection (e.g. Pedley et al. 1988) is reasonable. However, notice the qualitative differences between D_{xx} and D_{zz} around $\zeta = 0$. The typical measured value for $\mathcal{N}$ of 1.3 (Hill and Häder 1997) has a significant effect on the type of stationary point of D_{zz} and the sign of the gradient of D_{xz} at $\zeta = 0$ when compared to the case when $\mathcal{N} = 1.0$. In fact D_{xz} looks very flat, at this value of $\mathcal{N}$, for all ζ. Otherwise, increasing $\mathcal{N}$ increases the magnitude of the diagonal terms in the diffusion tensor.

10 Asymptotic results

In this section we consider the case where $\mathcal{N} = 1$ in order to compare the results from the spherical harmonic expansion with independently derived asymptotics. For the case where there is no flow, Pedley and Kessler (1990) calculate the diffusion tensor to be orthotropic, with components $D_H = 0.26$ and $D_V = 0.16$. For small vorticity Pedley and Kessler (1990) find (to

Table 1. Comparison of values of the diffusion tensor for varying approximation truncation order, ζ and $\mathcal{N}$, where $\chi = \xi = 0$

ζ	D_{xx}	D_{zz}	D_{xx}	D_{zz}
	$\mathcal{N} = 1.0$		$\mathcal{N} = 1.3$	
	2nd order approximation			
0.0	0.252	0.189	0.328	0.337
0.2	0.252	0.191	0.329	0.337
0.4	0.251	0.199	0.334	0.339
0.8	0.248	0.234	0.345	0.355
1.6	0.271	0.293	0.380	0.394
3.2	0.313	0.321	0.419	0.418
	3rd order approximation			
0.0	0.260	0.154	0.338	0.298
0.2	0.257	0.162	0.336	0.304
0.4	0.250	0.182	0.333	0.318
0.8	0.240	0.235	0.335	0.356
1.6	0.268	0.296	0.376	0.394
3.2	0.313	0.321	0.418	0.418
	4th order approximation			
0.0	0.259	0.156	0.337	0.301
0.2	0.257	0.163	0.336	0.306
0.4	0.250	0.182	0.334	0.319
0.8	0.241	0.234	0.336	0.355
1.6	0.268	0.296	0.376	0.396
3.2	0.313	0.321	0.418	0.418

2 significant figures)

$$\frac{\boldsymbol{D}}{V_s^2\tau} = \begin{pmatrix} 0.26 & 0 & -0.097\zeta \\ 0 & 0.26 & 0 \\ -0.097\zeta & 0 & 0.16 \end{pmatrix} + O(\zeta^2)\,. \tag{55}$$

Expanding Equation (28) for an 4th order truncation gives

$$\frac{\boldsymbol{D}}{V_s^2\tau} = \begin{pmatrix} 0.259 - 0.0709\zeta^2 & 0 & -0.102\zeta \\ 0 & 0.259 - 0.169\zeta^2 & 0 \\ -0.102\zeta & 0 & 0.156 + 0.181\zeta^2 \end{pmatrix} + O(\zeta^3)\,, \tag{56}$$

to 3 significant figures. The no flow values compare well with those given in Equation (55). The first correction to the diagonal terms occurs at $O(\zeta^2)$, in keeping with the expected symmetry, which are beyond those calculated by Pedley and Kessler (1990).

If we consider the case where vorticity is very large, $\zeta \gg 1$, then, for a spherical harmonic expansion at second order, the asymptotic expansions of

Equations (52) give

$$A_1^0 = 0.45455\frac{1}{\pi\zeta^2} + O\left(\frac{1}{\zeta^4}\right) \tag{57}$$

$$A_1^1 = 0.5\frac{1}{\pi\zeta} + O\left(\frac{1}{\zeta^3}\right) \tag{58}$$

$$A_2^0 = -0.29167\frac{1}{\pi\zeta^2} + O\left(\frac{1}{\zeta^4}\right) \tag{59}$$

$$A_2^1 = 0.56818\frac{1}{\pi\zeta^3} + O\left(\frac{1}{\zeta^5}\right) \tag{60}$$

$$A_2^2 = 0.10417\frac{1}{\pi\zeta^2} + O\left(\frac{1}{\zeta^4}\right), \tag{61}$$

to 5 significant figures. Substituting these functions into Equations (18) and (28) provides

$$\langle \boldsymbol{p} \rangle = \begin{pmatrix} 0.66666\frac{1}{\zeta} \\ 0 \\ 0.60606\frac{1}{\zeta^2} \end{pmatrix} + O\left(\frac{1}{\zeta^3}\right) \tag{62}$$

and

$$\frac{\boldsymbol{D}}{V_s^2\tau} = \frac{1}{3}\boldsymbol{I} + \begin{pmatrix} -0.2\frac{1}{\zeta^2} & 0 & 0.050500\frac{1}{\zeta^3} \\ 0 & -0.088893\frac{1}{\zeta^2} & 0 \\ 0.050500\frac{1}{\zeta^3} & 0 & -0.15556\frac{1}{\zeta^2} \end{pmatrix} + O\left(\frac{1}{\zeta^4}\right). \tag{63}$$

Asymptotic results for large ζ can be derived independently as follows. We begin again from the non-dimensionalised Fokker-Planck Equation (3), in which we consider spherical particles, thus setting $\alpha_0 = 0$. Taking $\lambda = O(1)$ and $\zeta \equiv \eta\omega \gg 1$ we form the small parameter $\delta = (\zeta\lambda)^{-1} \ll 1$. In order to present the asymptotic theory as generally as possible, we allow the vorticity to have a vertical component. We follow Brenner and Weissman (1972) in the choice of coordinate system by defining the unit vectors

$$\boldsymbol{e}_1 = (\hat{\boldsymbol{\omega}} \wedge \boldsymbol{k}) \wedge \hat{\boldsymbol{\omega}}/\sin\gamma\ , \tag{64}$$

$$\boldsymbol{e}_2 = \hat{\boldsymbol{\omega}} \wedge \boldsymbol{k}/\sin\gamma \tag{65}$$

and

$$\boldsymbol{e}_3 = \hat{\boldsymbol{\omega}} \tag{66}$$

where γ is the angle between the unit vorticity vector, $\hat{\boldsymbol{\omega}}$, and $\boldsymbol{k}$. ($\boldsymbol{e}_1$, $\boldsymbol{e}_2$, $\boldsymbol{e}_3$) defines a Cartesian coordinate system in which

$$\boldsymbol{k} = \sin\gamma\boldsymbol{e}_1 + \cos\gamma\boldsymbol{e}_3 \tag{67}$$

and

$$\boldsymbol{p} = \sin\theta\cos\phi\boldsymbol{e}_1 + \sin\theta\sin\phi\boldsymbol{e}_2 + \cos\theta\boldsymbol{e}_3\ . \tag{68}$$

Equation (3) becomes

$$\frac{\partial f}{\partial \phi} = \delta\Bigg\{\frac{1}{\sin\theta}\frac{\partial}{\partial\theta}\left(\sin\theta\frac{\partial f}{\partial\theta}\right) + \frac{1}{\sin^2\theta}\frac{\partial^2 f}{\partial\phi^2} + \lambda\Bigg[\frac{\sin\gamma\sin\phi}{\sin\theta}\frac{\partial f}{\partial\phi} - (\sin\gamma\cos\theta\cos\phi - \cos\gamma\sin\theta)\frac{\partial f}{\partial\theta} + 2(\sin\gamma\sin\theta\cos\phi + \cos\gamma\cos\theta) f\Bigg]\Bigg\}. \tag{69}$$

Expanding the orientational p.d.f. as

$$f = f_0 + \delta f_1 + \delta^2 f_2 + \cdots, \tag{70}$$

the leading order gives

$$\frac{\partial f_0}{\partial\phi} = 0. \tag{71}$$

Hence, $f_0 \equiv f_0(\theta)$, where $2\pi\int_0^\pi f_0(\theta)\sin\theta\, d\theta = 1$. At $O(\delta)$,

$$\frac{\partial f_1}{\partial\phi} = \frac{1}{\sin\theta}\frac{d}{d\theta}\left(\sin\theta\frac{df_0}{d\theta}\right) + \lambda\Bigg[-(\sin\gamma\cos\theta\cos\phi - \cos\gamma\sin\theta)\frac{df_0}{d\theta} + 2(\sin\gamma\sin\theta\cos\phi + \cos\gamma\cos\theta) f_0\Bigg]. \tag{72}$$

Now f_1 must be periodic in ϕ with period 2π so the terms independent of ϕ must vanish, i.e.

$$\frac{1}{\sin\theta}\frac{d}{d\theta}\left(\sin\theta\frac{df_0}{d\theta}\right) + \lambda\cos\gamma\left[\sin\theta\frac{df_0}{d\theta} + 2\cos\theta f_0\right] = 0, \tag{73}$$

which is an ordinary differential equation from which f_0 can be determined. Writing $x = \cos\theta$, we obtain

$$\frac{d}{dx}\left[(1-x^2)\frac{df_0}{dx}\right] + \lambda\cos\gamma\left[-(1-x^2)\frac{df_0}{dx} + 2x f_0\right] = 0 \tag{74}$$

subject to $\int_{-1}^{1} f_0(x)\, dx = 1/2\pi$. Hence,

$$f_0(\theta) = \mu e^{\lambda'\cos\theta}, \tag{75}$$

where $\lambda' = \lambda\cos\gamma$ and

$$\mu = \frac{\lambda'}{4\pi\sinh\lambda'}. \tag{76}$$

Integrating Equation (72) gives

$$f_1 = F_1(\theta) + \sin\phi G_1(\theta)\,, \tag{77}$$

where

$$G_1(\theta) = \mu\lambda e^{\lambda'\cos\theta}\sin\gamma\sin\theta(\lambda'\cos\theta + 2) \tag{78}$$

and

$$\int_0^\pi F_1(\theta)\sin\theta\,d\theta = 0\,. \tag{79}$$

At $O(\delta^2)$ we obtain

$$\frac{\partial f_2}{\partial\phi} = \frac{1}{\sin\theta}\frac{\partial}{\partial\theta}\left(\sin\theta\frac{\partial f_1}{\partial\theta}\right) + \frac{1}{\sin^2\theta}\frac{\partial^2 f_1}{\partial\phi^2}$$
$$+ \lambda\left[\frac{\sin\gamma\sin\phi}{\sin\theta}\frac{\partial f_1}{\partial\phi} - (\sin\gamma\cos\theta\cos\phi - \cos\gamma\sin\theta)\frac{\partial f_1}{\partial\theta}\right.$$
$$\left. + 2(\sin\gamma\sin\theta\cos\phi + \cos\gamma\cos\theta) f_1\right]. \tag{80}$$

Again, since f_2 is periodic in ϕ, the terms independent of ϕ must be zero, so

$$\frac{1}{\sin\theta}\frac{d}{d\theta}\left(\sin\theta\frac{dF_1}{d\theta}\right) + \lambda\cos\gamma\left[\sin\theta\frac{dF_1}{d\theta} + 2\cos\theta F_1\right] = 0\,. \tag{81}$$

The only solution satisfying Equation (79) is

$$F_1 = 0 \tag{82}$$

and thus Equation (80) gives

$$f_2 = F_2(\theta) - \cos\phi G_{21}(\theta) - \cos 2\phi G_{22}(\theta)\,, \tag{83}$$

where

$$G_{21}(\theta) = -\mu\lambda\sin\gamma e^{\lambda' x}(1 - x^2)^{1/2}(4 - \lambda'^2 + 8\lambda' x + 2\lambda'^2 x^2) \tag{84}$$

and

$$G_{22}(\theta) = \frac{\mu}{4}\lambda^2\sin^2\gamma\, e^{\lambda' x}(1 - x^2)(6 + 6\lambda' x + \lambda'^2 x^2)\,. \tag{85}$$

In a similar manner, at $O(\delta^3)$ we get

$$\frac{1}{\sin\theta}\frac{d}{d\theta}\left(\sin\theta\frac{dF_2}{d\theta}\right) + \frac{\lambda\sin\gamma}{2\sin\theta}G_{21} + \lambda\cos\gamma\left[\sin\theta\frac{dF_2}{d\theta} + 2\cos\theta F_2\right]$$
$$+ \lambda\sin\gamma\left[\frac{1}{2}\cos\theta\frac{dG_{21}}{d\theta} - \sin\theta G_{21}\right] = 0\,. \tag{86}$$

This expression can be integrated as it stands but, instead, we now take the limit $\gamma \to \pi/2$ (so as to compare with results from previous sections) so that

$\lambda' \to 0$ and $\mu \to 1/4\pi$. In this limit,

$$G_1(\theta) = \frac{\lambda}{2\pi} \sin\theta \,, \tag{87}$$

$$G_{21}(\theta) = -\frac{\lambda \sin\theta}{\pi} \tag{88}$$

and

$$G_{22}(\theta) = \frac{3\lambda^2 \sin^2\theta}{8\pi} \,. \tag{89}$$

Solving for F_2 yields

$$F_2(x) = \frac{\lambda^2}{12\pi}(1 - 3x^2) \,. \tag{90}$$

Therefore,

$$f_2 = \frac{\lambda^2}{12\pi}(1 - 3\cos^2\theta) + \frac{\lambda}{\pi}\cos\phi \sin\theta - \frac{3\lambda^2}{8\pi}\cos 2\phi \sin^2\theta \,. \tag{91}$$

Equations (15) and (26) allow us to calculate the average swimming direction, $\langle \boldsymbol{p} \rangle$, and the diffusion tensor, $\boldsymbol{D}$, respectively. Writing

$$\langle \boldsymbol{p} \rangle = \langle \boldsymbol{p} \rangle^{(0)} + \delta \langle \boldsymbol{p} \rangle^{(1)} + \delta^2 \langle \boldsymbol{p} \rangle^{(2)} + \ldots \tag{92}$$

we find that

$$\langle \boldsymbol{p} \rangle^{(0)} = \left(0, 0, \coth\lambda' - \frac{1}{\lambda'}\right) \to (0, 0, 0) \text{ as } \gamma \to \frac{\pi}{2} \,, \tag{93}$$

$$\langle \boldsymbol{p} \rangle^{(1)} = \left(0, \lambda \sin\gamma \left[1 + \frac{1}{\lambda'^2} - \frac{\coth\lambda'}{\lambda'}\right], 0\right) \to \left(0, \frac{2}{3\lambda}, 0\right) \text{ as } \gamma \to \frac{\pi}{2} \tag{94}$$

and

$$\langle \boldsymbol{p} \rangle^{(2)} \to \left(\frac{4\lambda}{3}, 0, 0\right) \text{ as } \gamma \to \frac{\pi}{2} \,. \tag{95}$$

In a similar manner,

$$\langle \boldsymbol{pp} \rangle = \frac{1}{3}\boldsymbol{I} + \delta^2\lambda^2 \begin{pmatrix} -\frac{7}{45} & 0 & 0 \\ 0 & \frac{11}{45} & 0 \\ 0 & 0 & -\frac{4}{45} \end{pmatrix} + O(\delta^3) \,. \tag{96}$$

(These results were quoted, without derivation, by Pedley and Kessler (1992), with an erroneous off-diagonal term in $\langle \boldsymbol{pp} \rangle$.) We may now translate these laboratory coordinates to the coordinates in the previous sections by the simple transformation,

$$(x_1, x_2, x_3) \to (x_3, -x_1, -x_2) \,. \tag{97}$$

In particular, if $\lambda = 2.2$ and $\mathscr{N} = 1.0$ then

$$\langle \boldsymbol{p} \rangle = \begin{pmatrix} 0.66667\frac{1}{\zeta} \\ 0 \\ 0.60606\frac{1}{\zeta^2} \end{pmatrix} + O\left(\frac{1}{\zeta^3}\right) \tag{98}$$

and

$$\frac{\boldsymbol{D}}{V_s^2\tau} = \langle \boldsymbol{pp} \rangle - \langle \boldsymbol{p} \rangle \langle \boldsymbol{p} \rangle \tag{99}$$

$$= \frac{1}{3}\boldsymbol{I} + \begin{pmatrix} -0.2\frac{1}{\zeta^2} & 0 & 0 \\ 0 & -0.088889\frac{1}{\zeta^2} & 0 \\ 0 & 0 & -0.15556\frac{1}{\zeta^2} \end{pmatrix} + O\left(\frac{1}{\zeta^3}\right) \tag{100}$$

to 5 significant figures. Both these expressions show excellent agreement with Equations (62) and (63).

11 Discussion

In this paper we have demonstrated that closed-form expressions can be obtained, in terms of the first five coefficients of the spherical harmonics, for the first two moments of the particle orientation.

For the case of spherical particles, where $\alpha_0 = 0$, the coefficients of the spherical harmonic expansion converge very rapidly. The second order approximation captures all of the behaviour (see Fig. 2), and yet is sufficiently simple to be used in a non-linear analysis of bioconvection where relatively compact expressions are benefical (Bees and Hill 1997b). The expansion to order three is almost indistinguishable from higher orders and the second order truncation deviates by less than 3% from the third order. Asymptotic expressions have been derived, independently of the spherical harmonic expansion, that capture the behaviour of the system for small and large vorticity. These expressions compare extremely well with the results from the spherical harmonic expansion, thus validating the methods used to derive both sets of results. We also show that the results can be extended to a three-dimensional flow field in which there is no vertical vorticity. This will aid future analysis on non-linear planform selection in bioconvection.

The case of aspherical particles, or non-zero α_0, is not so well behaved. For applications involving large ranges of rate-of-strain the method may not be the most efficient means of obtaining a solution as we require high orders of approximation and, hence, long expressions for the coefficients. This is due to the inevitable resolution problems associated with large straining motions constraining the cells to swim in well defined directions. However, for bioconvection problems, in which very large straining motions are never encountered, the method can be used with confidence. For a range of values for which rate-of-strain is small, convergence is rapid, and this range increases in size as the order of the approximation is increased. To extend the range further one could construct simple, smooth functions from the convergent regions of the coefficients and asymptotes for dominant flow conditions (e.g. for large rate-of-strain).

Finally, the methods described in this paper are sufficiently flexible that solutions could be obtained for combinations of taxes (or orientational responses to external stimuli). In particular, the interaction of gravitaxis, gyrotaxis and phototaxis (see Kessler et al. 1992) could be investigated.

MAB would like to acknowledge the financial support of the EPSRC through an Earmarked Studentship in Mathematical Biology during this work.

Appendix

Below is a summary of the operations or recursion relations that are used in this paper. These relations allow expressions on the LHS to be written in a simpler functional form (RHS). Each of these expressions is derived from the identities quoted by Arfken (1985). Here, P_n^m are associated Legendre polynomials and T_n^m are expressions of associated Legendre polynomials that can be labeled with the indices m and n.

- X_c:

$$xP_n^m \equiv \frac{n+m}{2n+1} P_{n-1}^m + \frac{n-m+1}{2n+1} P_{n+1}^m \tag{101}$$

$$X_c(T_n^m)\colon\ T_n^m \mapsto \frac{n+m}{2n+1} T_{n-1}^m + \frac{n-m+1}{2n+1} T_{n+1}^m\ . \tag{102}$$

- X_{ss}:

$$X_{ss}(T_n^m)\colon\ T_n^m \mapsto T_n^m - X_c(X_c(T_n^m))\ . \tag{103}$$

- X_{ssp}:

$$(1-x^2) P_n^{m\prime} \equiv \frac{1}{2n+1}\left((n+m)(n+1) P_{n-1}^m - n(n-m+1) P_{n+1}^m\right) \tag{104}$$

$$X_{ssp}(T_n^m)\colon\ T_n^m \mapsto \frac{1}{2n+1}\left((n+m)(n+1) T_{n-1}^m - n(n-m+1) T_{n+1}^m\right)\ . \tag{105}$$

- X_{su}:

$$(2n+1)\sqrt{1-x^2} P_n^m \equiv P_{n+1}^{m+1} - P_{n-1}^{m+1} \tag{106}$$

$$X_{su}(T_n^m)\colon\ T_n^m \mapsto T_{n+1}^{m+1} - T_{n-1}^{m+1}\ . \tag{107}$$

- X_{sd}:

$$(2n+1)\sqrt{1-x^2} P_n^m \equiv (n+m)(n+m-1) P_{n-1}^{m-1} - (n-m+1)(n-m+2) P_{n+1}^{m-1} \tag{108}$$

$$X_{sd}(T_n^m)\colon\ T_n^m \mapsto (n+m)(n+m-1) T_{n-1}^{m-1} - (n-m+1)(n-m+2) T_{n+1}^{m-1}\ . \tag{109}$$

- X_{spu}:

$$\sqrt{1-x^2}P_n^{m\prime} \equiv P_n^{m+1} - \frac{mx}{\sqrt{1-x^2}} P_n^m \tag{110}$$

$$X_{spu}(T_n^m)\colon\ T_n^m \mapsto T_n^{m+1} - \frac{mx}{\sqrt{1-x^2}} T_n^m\ . \tag{111}$$

- X_{spd}:

$$\sqrt{1-x^2}P_n^{m\prime} \equiv -(n-m+1)(n+m)\ P_n^{m-1} + \frac{mx}{\sqrt{1-x^2}} P_n^m \tag{112}$$

$$X_{spd}(T_n^m)\colon\ T_n^m \mapsto -(n-m+1)(n+m)\ T_n^{m-1} + \frac{mx}{\sqrt{1-x^2}} T_n^m\ . \tag{113}$$

- $X_{\sin}$:

$$S^1S^m \equiv \tfrac{1}{2}C^{m-1} - \tfrac{1}{2}C^{m+1} \tag{114}$$

$$X_{\sin}(S^1S^m)\colon\ S^1S^m \mapsto \tfrac{1}{2}C^{m-1} - \tfrac{1}{2}C^{m+1}\ . \tag{115}$$

$X_{\cos}$:

$$C^1C^m \equiv \tfrac{1}{2}C^{m-1} + \tfrac{1}{2}C^{m+1}\ . \tag{116}$$

$$X_{\cos}(C^1C^m)\colon\ C^1C^m \mapsto \tfrac{1}{2}C^{m-1} + \tfrac{1}{2}C^{m+1}\ . \tag{117}$$

References

G. Arfken, Mathematical methods for Physicists. Academic Press Inc., London, 3rd ed., 1985

M. A. Bees, Non-Linear Pattern Generation in Suspensions of Swimming Micro-organisms. PhD thesis, University of Leeds, 1996

M. A. Bees and N. A. Hill, Wavelengths of Bioconvection Patterns. Journal of Experimental Biology, **200**: 1515–1526, 1997a

M. A. Bees and N. A. Hill, Non-Linear Bioconvection in a deep suspension of gyrotactic micro-organisms. Journal of Mathematical Biology (submitted), 1997b

H. Brenner and M. H. Weissmann, Rheology of a dilute suspension of dipolar spherical particles in an external field. II. Effects of rotary brownian motion. Journal of Colloid and Interface Science, **41**(3): 499–531, December 1972

S. Childress, M. Levandowsky and E. A. Spiegel, Pattern formation in a suspension of swimming micro-organisms: equations and stability theory. Journal of Fluid Mechanics, **69**: 595–613, 1975

N. A. Hill and D. -P. Häder, A biased random walk model for the trajectories of swimming micro-organisms. Journal of Theoretical Biology, **186**: 503–526, 1997

N. A. Hill, T. J. Pedley and J. O. Kessler, Growth of bioconvection patterns in a suspension of gyrotactic micro-organisms in a layer of finite depth. Journal of Fluid Mechanics, **208**: 509–543, 1989

E. J. Hinch and L. G. Leal, The effect of Brownian motion on the rheological properties of a suspension of non-spherical particles. Journal of Fluid Mechanics, **52**: 683–712, 1972a

G. B. Jeffrey, The motion of ellipsoidal particles immersed in a viscous fluid. Proceedings of the Royal Society of London, **A102**: 161–179, 1922

M. S. Jones, L. le Baron and T. J. Pedley, Biflagellate gyrotaxis in a shear flow. Journal of Fluid Mechanics, **281**: 137–158, 1994

J. O. Kessler, Gyrotactic buoyant convection and spontaneous pattern formation in algal cell cultures In M. G. Velarde, editor, Non-equilibrium cooperative phenomena in physics and related fields, pages 241–248. New York: Plenum, 1984
J. O. Kessler, Co-operative and concentrative phenomena of swimming micro-organisms. Contempory Physics, **26**(2): 147–166, 1985
J. O. Kessler, Individual and collective dynamics of swimming cells. Journal of Fluid Mechanics, **173**: 191–205, 1986
J. O. Kessler, N. A. Hill and D. P. Häder, Orientation of swimming flagellates by simultaneously acting external factors. Journal of Phycology, **28**: 816–822, 1992
L. G. Leal and E. J. Hinch, The rheology of a suspension of nearly spherical particles subject to Brownian rotations Journal of Fluid Mechanics, **55**: 745–765, 1972
K. Mardia. Statistics of directional data, Academic Press, 1972
T. J. Pedley and J. O. Kessler, A new continuum model for suspensions of gyrotactic micro-organisms. Journal of Fluid Mechanics **212**: 155–182, 1990
T. J. Pedley and J. O. Kessler, Hydrodynamic phenomena in suspensions of swimming micro-organisms. Annual Review of Fluid Mechanics, **24**: 313–358, 1992
J. R. Platt, "Bioconvection patterns" in cultures of free-swimming organisms. Science, **133**: 1766–1767, 1961
O. Savas, On flow visualization using reflective flakes. Journal of Fluid Mechanics, **152**: 235–248, 1985
S. R. Strand and S. Kim, Dynamics and rheology of a dilute suspension of dipolar nonspherical particles in an external field: Part 1. Steady shear flows, Rheological Acta, **31**: 94–117, 1992